Chaotic Motions and Fault Detection in a Cracked Rotor

P. C. MÜLLER, J. BAJKOWSKI, and D. SÖFFKER
Safety Control Engineering, University of Wuppertal, Germany

Abstract. Applying the theory of Lyapunov exponents for nonsmooth dynamical systems, chaotic motions and strange attractors are found in the case of a cracked rotor. To detect the crack and establish a clear relation between shaft cracks in turbo rotors and induced phenomena in vibrations measured in bearings, a model-based method is applied. Based on a fictitious model of the time behaviour of the nonlinearities, a state observer of an extended dynamical system is designed resulting in estimates of the nonlinear effects.

Key words: Chaos, reconstruction of nonlinearities, observer, fault diagnosis.

1. Introduction

In this paper the nonlinear dynamics of a cracked rotating shaft is investigated. The nonlinear effects are caused by the crack, which is described by changing stiffness coefficients, so the system becomes one that is parametrically excited and nonlinear (with discontinuities caused by transitions between motion without crack and motion with crack).

It is well known that nonsmooth systems can exhibit different types of motion, even chaotic behaviour. Engineering problems of this type where chaos was found numerically and/or experimentally are, for example: a rotor touching a boundary, cf. Szczygielski [1], Bajkowski and Müller [2]; a vibrating beam with an amplitude-constraining stop, cf. Moon and Shaw [3]; rattling gear drives, cf. Pfeiffer, [4]; dynamics of railway vehicles in De Pater [5, 6], Meijaard [7]; dynamics of a section of a drillstring, cf. Jansen [8]; a constrained pipe conveying fluid, cf. Paidoussis and Moon [9]; oscillations of structures due to dry friction, cf. Popp and Stelter [10], Stelter [11]; and a cracked Laval rotor, cf. Fritzen [12].

Unfortunately, these systems cannot be directly analyzed by methods which require certain smoothness assumptions on the nonlinear functions involved. Therefore, it is shown that a generalized method can be applied if some care is devoted to the handling of the discontinuities, cf. Müller *et al.* [13].

A detailed study of the vibrational behaviour of a cracked rotating shaft is an important problem for engineers working in the area of machine dynamics. Recent investigations of oscillations induced by cracks have been shown that beside the well-known limit cycle behaviour, chaotic motions are also possible, depending on the system parameters, i.e. crack depth or damping coefficients, cf. Fritzen [12], Söffker *et al.* [14]. Also the authors developed in [15] a new concept of the analysis and of the fault detection of cracked rotors which are improved in this paper including a model based calculation of Lyapunov exponents and a different fault detection fault model.

It is very difficult to conclude the existence of a shaft crack, because there is no clear relation between the crack and the caused phenomena. In this way the main problem is to establish a clear and unambiguous relation between the crack and the caused phenomena.

The classical methods consist of measurements taken of oil temperatures in bearings or control of the vibration peaks with regard to maximum allowed values. Also, coastdown-measurements are done (Zimmer and Bently [16]). For all these ways the experience of the machine operator is very important, because none of the classical methods provides an obvious statement about the crack.

The modern methods for failure detection are called Vibration Monitoring Systems (VMS). For these, FFT- and Cepstrum Analysis are done, and also statistical methods and/or pattern recognition are used (Peter [17]; Ericsson, [18]). These methods have a great potential, because it is possible to use them without dismounting any part of the machine or even stopping the machine.

There are a lot of crack models, but the typical effect of the crack is already described by the simplest one. This typical behaviour is the breathing of the crack, and is modelled by the 'Hinge-Mechanism' of Gasch [19]. Henry and Okah-Avae [20] considered the non-linear mechanism of a breathing crack with different elasticities for open and closed crack, described in body-fixed rotating coordinates. Mayes and Davies [21] correlated some experimental results with their theoretical background and suggested a method for calculating the changing stiffness due to a crack. Grabowski and Mahrenholtz [22] used modal formulations to investigate the vibrational behaviour of realistic cracked rotor systems. They developed a crack mechanism and used it in their dynamic rotor model. Bently [23, 24] and Muszynska [25] investigated the dynamics of cracked systems by the development of both demonstration rigs and practicable crack detection systems based on their own theoretical work. Currently, the vibrations of cracked rotors and the detection of cracks are active fields of research, e.g., Schmalhorst [26], Wauer [27] and Papadopoulos and Dimarogonas [28, 29].

Here, the new method [14, 15, 30] based on the theory of disturbance rejection control, extended for nonlinear systems and applied to a turbo rotor, is presented. In this way the crack is interpreted as an external disturbance. Due to the theory of estimating unknown disturbances of a dynamic system, simple measurements of displacements and/or velocities – obtained from simulation or experiment – are used to generate additional time signals by state observers to obtain estimates of the non-linear effects. The state observer is based on the known part of the vibration system and a linear fictitious model approximating the crack. Calculating the relative crack compliance as the ratio of additional compliance caused by the crack and undamaged compliance, a clear statement is possible about the opening and closing, and therefore for the existence of the crack, and about the crack depth. In opposite to [15] here the simulated signals are corrupted by noise to approximate closely real rotor systems.

This paper is organized as follows. The general equations of motion and crack phenomena will be presented in Section 2. In Section 3 a linearization of nonsmooth dynamical systems and transition conditions and its application to the rotor as a lumped-mass-model of 7 beam elements and 16 degrees of freedom, behaviour of the system depending on the parameter, chaotic motion and strange attractors are presented. Section 4 is related to the crack detection method by state observers (pole assignment and Riccati observer) in the case of turbo rotors.

2. Equations of Motion

The nonlinear equations of motion for the rotating cracked shaft are described by

$$\mathbf{M}\ddot{\mathbf{z}} + (\mathbf{D} + \mathbf{G})\dot{\mathbf{z}} + \mathbf{K}\mathbf{z} = \mathbf{f}(t) + \mathbf{N}_n\mathbf{h}(\mathbf{z}(t), t) \tag{1}$$

with

$\mathbf{z}, \dot{\mathbf{z}}, \ddot{\mathbf{z}}$: displacement vector and its time derivatives of order n,

$\mathbf{M}$: mass matrix,

$\mathbf{D}, \mathbf{G}$: matrices of damping and gyroscopic effects,

$\mathbf{K}$: stiffness matrix,

$\mathbf{f}(t)$: vector of unbalances,

$\mathbf{N}_n$: input matrix of nonlinearities, and

$\mathbf{h}(\mathbf{z}(t), t)$: vector of nonlinearities caused by the crack.

The vector $\mathbf{h}(\mathbf{z}(t), t)$ contains the specific forces caused by the crack. To consider the crack influence in the equations of motion (1) a crack model is needed in the way that it describes the change in stiffness and/or damping coefficients, e.g., by a crack element stiffness or damping matrix. Usual crack models (Gasch, [19]; Schmalhorst, [26]) use the change in stiffness coefficients, according to equations (2)–(4) as:

$$\mathbf{h} = \begin{cases} \mathbf{0} & : \text{in the case of no crack or closed crack} \\ \left[0_1 \ldots 0_i \; \mathbf{h}^T{}_{chcr}(\tilde{\mathbf{z}}(t), t) \; 0_{i+1+e_n} \ldots 0_n \right]^T & : \text{in the case of open crack} \end{cases} \tag{2}$$

with

$$\mathbf{h}_{chcr}(\tilde{\mathbf{z}}(t), t) = \mathbf{K}_e [z_i \ldots z_{i+e_n}]^T, \tag{3}$$

$$\mathbf{K}_e = \begin{bmatrix} a_{11} & \cdots & a_{1e_n} \\ \vdots & \ddots & \vdots \\ a_{e_n 1} & \cdots & a_{e_n e_n} \end{bmatrix} \text{ with } a_{ij} = a_{ji}, \tag{4}$$

where $\mathbf{K}_e$ represents a general additional crack stiffness matrix of order e_n. Therefore the nonlinear crack behaviour is described by a piecewise linear characteristic where the switching depends on the system state.

In the literature (Wauer, [27]) a lot of crack models are mentioned, which are very sensitive, especially the FEM-crack model of Schmalhorst [26]. But the typical behaviour of the crack, the 'breathing' of the crack under weight influence, is already described by the very simple model of Gasch [19]. The crack model of Gasch, Figure 1, is described in the rotating coordinate system by

$$\begin{bmatrix} \xi \\ \eta \end{bmatrix} = \begin{bmatrix} h + h_a & 0 \\ 0 & h \end{bmatrix} \begin{bmatrix} F_\xi \\ F_\eta \end{bmatrix}. \tag{5}$$

The compliance h in the crack direction ξ will be increased with an additional compliance h_a in case of an open crack, which depends on the crack depth. The relative crack compliance h_r as the ratio
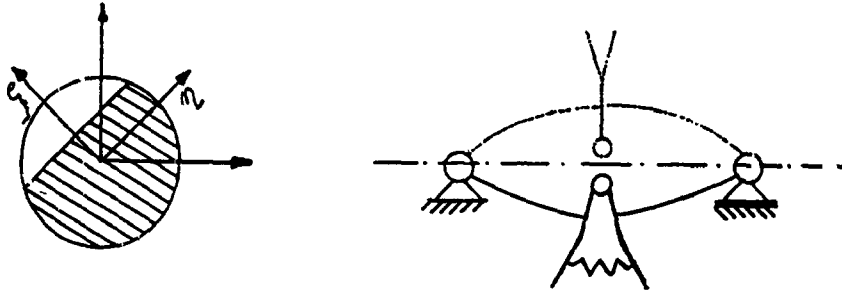
$$h_r = \frac{h_a}{h} \tag{6}$$

Fig. 1. Illustration of crack model of Gasch [19].

is established by experimental investigations of Mayes and Davies [31] for different crack depths. For very small cracks the values are approximated. The opening-condition of the crack can be formulated via the curvature at the crack position (ξ'', ξ''_{i}), or approximately via the displacements near the crack $(\xi_{i-e_n}, \xi_{i+e_n})$

$$\xi_i > \frac{\xi_{i-e_n} + \xi_{i+e_n}}{2}, \quad \text{or} \quad \chi = \chi_i = \xi_i - \frac{\xi_{i-e_n} + \xi_{i+e_n}}{2} > 0 \tag{7}$$

where $e_n = 2$ and χ is the opening condition for the crack.
Using the transformation matrix

$$\mathbf{T} = \left[\begin{array}{cc} \cos(\Omega t + \beta) & \sin(\Omega t + \beta) \\ -\sin(\Omega t + \beta) & \cos(\Omega t + \beta) \end{array} \right] \tag{8}$$

the element-stiffness-matrix $\mathbf{K}_e\,(\tilde{z}\,(t)\,,t)$ for a discretized model like an MBS-formulation in the inertial coordinate system looks like

$$\mathbf{K}_e = \frac{-h_r}{h(1 + h_r)} \left[\begin{array}{cc} \sin^2(\Omega t + \beta) & \sin(\Omega t + \beta)\cos(\Omega t + \beta) \\ \sin(\Omega t + \beta)\cos(\Omega t + \beta) & \cos^2(\Omega t + \beta) \end{array} \right] \tag{9}$$

where $\mathbf{K}_e$ depends on the opening condition (7) for the crack and on time, so the system in the inertial coordinates becomes a nonlinear and parametrically excited one.

3. Behaviour of the Cracked Rotor

There exist several quantitative and qualitative measures for the characterization of the system behaviour (attractors), e.g., phase plane plots, Poincaré sections, FFT-analysis, different kinds of dimensions and entropies (Lichtenberg and Lieberman [32], Moon [33]). Lyapunov exponents are chosen here to classify the system behaviour. As is well known, Lyapunov exponents measure the exponential rates of divergence or convergence of neighbouring trajectories associated with an attractor of a system (Oseledec [34], Eckmann and Ruelle [35], Haken [36]). For periodic attractors one obtains only negative and zero exponents indicating convergence to a highly predictable motion, whereas a chaotic system will exhibit at least one positive exponent. A positive exponent is significant because it gives an indication of the rate at which one loses the ability to predict the system response. This is closely tied to the property of sensitive dependence on initial conditions which is present in chaotic systems. Therefore, one way to determine if a system is behaving in a chaotic manner is to calculate

the Lyapunov exponents. The calculation of Lyapunov exponents is well developed, and a lot of references are available on this subject (Wolf *et al.* [37], Shimida and Nagashima [38], Benettin *et al.* [39]).

Usually the calculation of the exponents is performed considering an observed trajectory x(t), which can be considered as a solution of a certain dynamical system

$$\dot{\mathbf{x}} = \mathbf{f}(\mathbf{x}) \tag{10}$$

defined in an n-dimensional phase space, where $\mathbf{f} \in C^1$ is a differentiable vector function. On the other hand, the time evolution of a tangent vector $\delta\mathbf{x}$ in a tangent space at $\mathbf{x}(t)$ is represented by linearizing equation (10) over the trajectory of the original nonlinear equations,

$$\delta\dot{\mathbf{x}} = \mathbf{F}(t)\,\delta\mathbf{x} \tag{11}$$

where

$$\mathbf{F}(t) = \left.\frac{\partial \mathbf{f}}{\partial \mathbf{x}^T}\right|_{\mathbf{x}(t)} \tag{12}$$

is the Jacobian of $\mathbf{f}$. The spectrum of Lyapunov exponents σ_i for given starting position is

$$\sigma_i = \overline{\lim_{t\to\infty}} \frac{1}{t} \, ln \, \frac{\|\delta\mathbf{x}(t)\|}{\|\delta\mathbf{x}(t_0)\|}. \tag{13}$$

There are n Lyapunov exponents in the spectrum of an attractor on an n-dimensional dynamical system.

The algorithms [37, 38, 39] for computing Lyapunov exponents are directly applicable for smooth dynamical systems, but not in the case of mechanical systems with discontinuities [1–12]. For this aspect it is shown that a general method can be applied to compute the exponents, if some care is taken to the handling of the discontinuities. The linearized equations have to be supplemented with transition function conditions, and these allow one to determine the spectrum of Lyapunov exponents in the case of nonlinear systems with discontinuities, cf. Müller *et al.* [13].

3.1. THE LINEARIZED EQUATIONS AND TRANSITION EQUATIONS

In the case of a cracked rotor the following kinds of motion are possible:

(a) Motion without crack ('closed' crack, i.e. if $\chi \leq 0$ in equation (7)): The equations of motion can be rewritten in a state space form as

$$(t_0) \leq t < t_1 \ : \ \dot{\mathbf{x}} = \mathbf{f}_1(\mathbf{x}), \quad \mathbf{f}_1(\mathbf{x}) = \mathbf{A}\mathbf{x} + \mathbf{b}(t), \quad \mathbf{x}(t_0) = \mathbf{x}_0 \tag{14}$$

where $\mathbf{x}$ denotes the state vector, $\mathbf{A}$ is the system matrix, $\mathbf{b}$ represents the vector of excitation functions, and t_1 is the time for the switching point of the crack ($\chi = 0$).

(b) The transition from motion without crack to motion with crack, at time $t = t_1$,

$$t_1 \ : \ \chi_i(\mathbf{x}) = 0. \tag{15}$$

The transition condition at χ_i can be rewritten as

$$\mathbf{x}(t_{1+}) = \mathbf{g}(\mathbf{x}(t_{1-}))$$
(16)

where t_{1+}, t_{1-} are the right and the left limits at time t_1, respectively, and $\mathbf{g}(\mathbf{x})$ are the transition conditions.

(c) Motion with crack ('open' crack ($\chi_i > 0$) in equation (7)): The equations of motion are as follows:

$$(t_1) < t : \dot{\mathbf{x}} = \mathbf{f}_2(\mathbf{x}), \quad \mathbf{x}(t_1) = \mathbf{x}(t_{1+}),$$
$$\mathbf{f}_2(\mathbf{x}) = \mathbf{A}\,\mathbf{x} + \mathbf{b}(t) + \mathbf{N}\,\mathbf{n}(\mathbf{x}(t), t)$$
(17)

where $\mathbf{N}$ is the input matrix of nonlinearities, and $\mathbf{n}(\mathbf{x}(t), t)$ is the vector of nonlinear functions.

The equations of motion are piecewise smooth and a unique smooth solution exists on each interval between transitions.

For the numerical calculations, the linearized equations are needed. In the case of the 'closed' crack the linearized equations follow directly from (14) as

$$t_0 \leq t < t_1 : \delta\dot{\mathbf{x}} = \mathbf{F}_1(t)\,\delta\mathbf{x}, \quad \delta\mathbf{x}(t_0) = \delta\mathbf{x}_0, \quad \mathbf{F}_1(t) = \left.\frac{\partial \mathbf{f}_1}{\partial \mathbf{x}^T}\right|_{\mathbf{x}(t)}.$$
(18)

In the case of the 'open' crack the linearized equations follow as

$$t_1 < t : \delta\dot{\mathbf{x}} = \mathbf{F}_2(t)\,\delta\mathbf{x}, \quad \delta\mathbf{x}(t_1) = \delta\mathbf{x}_+, \quad \mathbf{F}_2(t) = \left.\frac{\partial \mathbf{f}_2}{\partial \mathbf{x}^T}\right|_{\mathbf{x}(t)}.$$
(19)

The transition from the one to the other case has to be considered within the linearization procedure, too, leading to linearized transition conditions [13]. According to [?] in case of transition from (14, 18) to (17, 19), ($\chi_i = 0$, at time $t = t_1$):

$$\delta\mathbf{x}_+ = -\left\{ \mathbf{G}(\mathbf{x}_-) + [\mathbf{G}(\mathbf{x}_-)\mathbf{f}_1(\mathbf{x}_-) - \mathbf{f}_2(\mathbf{x}_+)] \frac{\mathbf{H}\mathbf{x}_-}{\mathbf{H}(\mathbf{x}_-)\mathbf{f}_1(\mathbf{x}_-)} \right\} \delta\mathbf{x}_-,$$
(20)

$$\delta\mathbf{x}_- = \delta\mathbf{x}(\mathbf{t}_{1-}),$$
(21)

where

$$\mathbf{H}(\mathbf{x}_-) = \left.\frac{\partial \chi_i}{\partial \mathbf{x}}^T\right|_{\mathbf{x}_-} = \mathbf{c}^T,$$
(22)

$$\mathbf{G}(\mathbf{x}) = \frac{\partial \mathbf{g}}{\partial \mathbf{x}^T} = \mathbf{E} - \text{transition matrix},$$
(23)

$$\delta\mathbf{x}_- : \text{ end state for } t = t_{1-}$$
(24)

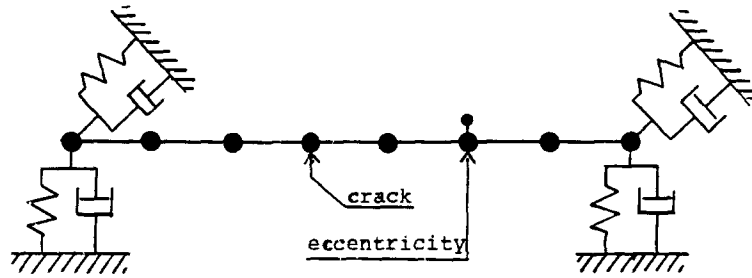$$\delta\mathbf{x}_+ : \text{ end state for } t = t_{1+}.$$
(25)

(26)

Fig. 2. Simple rotor.

3.2. EXAMPLE

The rotor used for theoretical investigations and simulations is described by the following assumptions, cf. Figure 2:

Rotor as a lumped-mass-model: 7 beam elements, length $l = 600\,mm$; radius $r = 140\,mm$; frequency $\Omega = 100\,\pi\ rad/s$; eccentricity $e_m = 0.02\,mm$; stiffness of bearings $k_s = 750$ kN/mm; damping as $D = \alpha_{mod}\,M + \beta_{mod}\,K$, $\alpha_{mod} = 0$, $\beta_{mod} = 0.00001$; number of degrees of freedom $n = 16$; number of nonlinearities $f = 2$; number of measurements $m = 8$ (measurements only in bearings as displacements and their velocities).

The system matrices are given in the Appendix.

In this case the crack indicator χ_i is defined as

$$\chi_i(\mathbf{x}) = \mathbf{c}^T \mathbf{x} \tag{27}$$

where

$$\mathbf{c}^T = [0 \quad 0 \quad 0 \quad 0 \quad -\frac{1}{2}\cos\phi \quad -\frac{1}{2}\sin\phi \quad \cos\phi$$

$$\sin\phi \quad -\frac{1}{2}\cos\phi \quad -\frac{1}{2}\sin\phi \quad \underbrace{0 \cdots 0}_{22\ \text{times}}], \qquad \phi = \Omega t + \beta. \tag{28}$$

The transition conditions (16) and the transition matrix (23) are:

$$g(\mathbf{x}) = \mathbf{E}\,\mathbf{x} \tag{29}$$

$$\mathbf{G}(\mathbf{x}) = \mathbf{E}. \tag{30}$$

Using (20), the following transitions for the linearized equations at $t = t_1$ are:

1. In the case 'closed' $\rightarrow$ 'open' crack:

$$\delta\mathbf{x}_+ = \delta\mathbf{x}_- - \mathbf{S}\,\mathbf{x}_-\frac{\mathbf{c}^T\,\delta\mathbf{x}_-}{\mathbf{c}^T\,\mathbf{A}\,\mathbf{x}_-}, \tag{31}$$
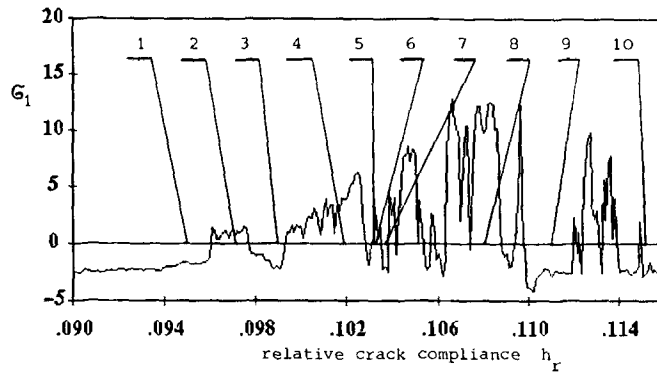
2. in the case 'open' $\rightarrow$ 'closed' crack:

Fig. 3. The greatest Lyapunov exponent-function of relative crack compliance for constant damping coefficient β_{mod} = 0.00001 (calculated after Wolf et al. [37]).

$$\delta \mathbf{x}_+ = \delta \mathbf{x}_- + \mathbf{S}\,\mathbf{x}_- \frac{\mathbf{c}^T \delta x_-}{\mathbf{c}^T \mathbf{A}\,\mathbf{x}_-}, \tag{32}$$

where

$$s_{ij} = 0, i, j = 1, 2, ..., 32, \text{except}$$

$$s_{23,7} = -k\cos^2(\Omega t + \beta)$$

$$s_{23,8} = -k\cos(\Omega t + \beta)\sin(\Omega t + \beta)$$

$$s_{24,7} = -k\sin(\Omega t + \beta)\cos(\Omega t + \beta)$$

$$s_{24,8} = -k\sin^2(\Omega t + \beta).$$

The Lyapunov exponents were calculated by making use of the algorithms given in [37]. To implement this procedure, the nonlinear equations of motion are integrated for some post-transient initial conditions (here 32 differential equations). Simultaneously, the linearized equations of motion are integrated for $2n$ different initial conditions, (here $32 \times 32 = 1024$ differential equations), defining an arbitrarily oriented frame of $2n$ orthonormal vectors. Because of the order of the system, $(32 + 1024)$, only the greatest Lyapunov exponent σ_1 was calculated as a function of relative crack compliance h_r. The results are shown in Figure 3.

To characterize the dynamic behaviour of the system besides Lyapunov exponents, Poincaré maps, phase plane plots, time responses and power spectra are used. The Poincaré maps presented in this work are defined at $t = 0$ (mod $(2\pi/\Omega)$), where Ω is the frequency of the parametric excitations. As the crack coefficient h_r is varied, different types of motion are observed, Figures 4, 4a, and 4j show phase plane plots, Poincaré sections, time histories and power spectrum for the ultrasubharmonic motion of order 3/2 (points 1, $h_r = 0.095$, and 10, $h_r = 0.115$, in Figure 3, respectively). For certain regions in the parameter space, as the parameter h_r is varied, the periodic motions become unstable and bifurcate, giving rise to stable quasiperiodic motions. The Poincaré map of a quasiperiodic motion is a closed curve in the phase plane, and are shown in Figures 4c and 4f (points 3, $h_r = 0.099$ and 6, $h_r = 0.1032$, in Figure 3, respectively). The transition from quasiperiodic motion to chaotic motion have been marked by appearance of fractal-like torus in phase space (Muntean and Moon [40]),

and is shown in Figures 4b and 4c, respectively (point 2, h_r=0.097, and point 4, h_r=0.102, in Figure 3). For certain values of h_r these quasiperiodic motions become unstable and bifurcate, giving rise to chaotic motions, Figure 4h (h_r =0.108 and point 8 in Figure 3). And finally Figures 4e, 4g, and 4i show different types of subharmonic motion of the order 1/5, 1/4 and 1/2, respectively (points 5, h_r = 0.103, 7, h_r = 0.1037, and 9, h_r = 0.111, in Figure 3). It is also interesting to examine the effect of the damping. For a constant crack depth, h_r = 0.102, we can obtain periodic, quasi-periodic, fractal-like torus or chaotic motions, Figure 5.

4. State Observers for Reconstruction of Nonlinear Effects

4.1. THE METHOD

Usual crack detection methods are based on signal analysis. As information only vibration signals are used. Further information about the mechanical system and about the fault we are looking for are not necessary. The method suggested in this paper is an observer-based method, so further information is needed besides the measurable signals, e.g., the mechanical model of the rotor and the characteristics about the typical behaviour of the crack. The principal way with a first application of this observer based method is taken in Söffker *et al.* [14].

Applying state space notation, equation (1) is described by

$$\dot{x} = Ax + b(t) + Nn(x(t)),$$
$$y = Cx. \tag{33}$$

Here x denotes the $2n$-dimensional state vector (consisting of displacement and velocity variables), A is the $2n \times 2n$ system matrix, and b represents the $2n$-dimensional vector of control inputs and/or excitation functions. The $2n \times f$ matrix N is the input matrix of the nonlinearities into the linear dynamical system. The vector $n(x(t), t)$ characterizes the f-dimensional vector of nonlinear functions. The m-dimensional vector y represents the measurements via the $m \times 2n$-dimensional matrix of measurements C. It is assumed that the system parameters (A, N, C) as well as the input and output time signals (b, y) are known. The task is to reconstruct the unknown nonlinearities (here the external disturbance forces of the crack)

$$n(x(t), t) \approx \hat{n}(\hat{x}(t)) \tag{34}$$

by applying state observers.

4.2. THE STATE OBSERVER

For consideration of external disturbances, the state space vector will be extended by a fictitious disturbance vector $v(t)$,

$$n(x(t)) \approx Hv(t),$$
$$\dot{v}(t) = Fv(t) + Gb(t), \tag{35}$$
$$\dim v = s,$$

to describe approximately the time behaviour of the nonlinearities. The model matrices F, G and H must be chosen in accordance with the technical background about the system. Here
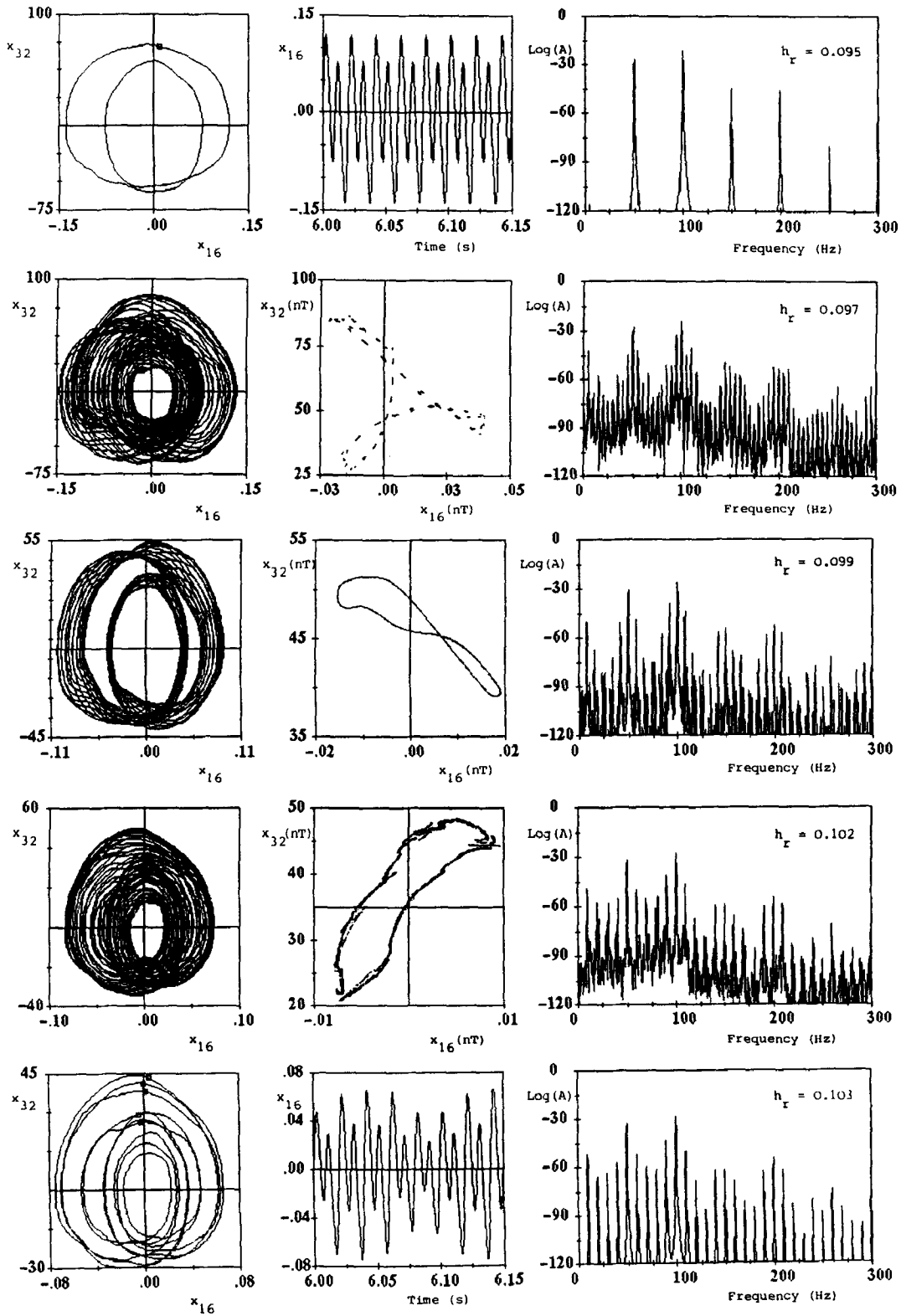
Fig. 4. Projection onto the (x_{16}, x_{32})-plane (right bearing, horizontal direction) of the trajectory, (the square indicates the limit set of Poincaré map with $t_0 = 0$; $T = 2\pi\Omega$, $\Omega = 50Hz$, $n = 10000$); time history and its corresponding power spectrum $(A = 20 \log \sqrt{Im_{16}^2 + Re_{16}^2})$, for different relative crack compliance h_r and constant damping coefficient $\beta_{mod} = 0.00001$.
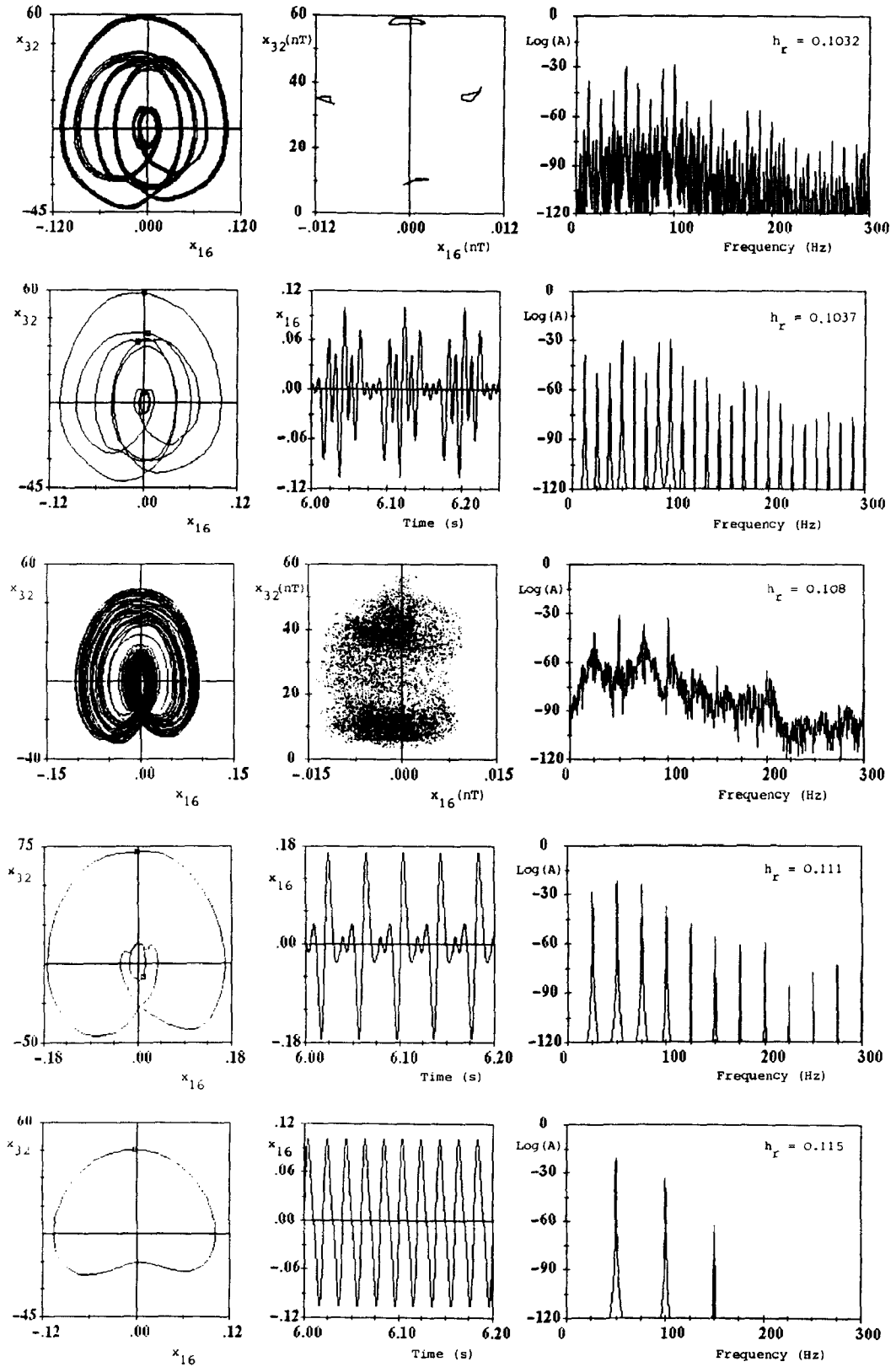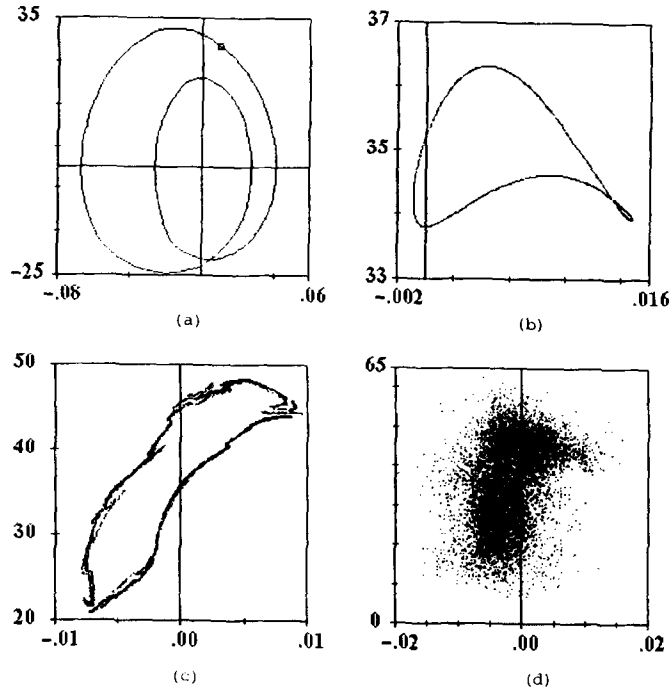
Fig. 4 (continued)

Fig. 5. Projection onto the (x_{16}, x_{32}) plane, (right bearing, horizontal direction), Poincaré map $(t_0 = 0, T = 2\pi/\Omega, \Omega = 50Hz, n = 10000)$, for different damping coefficient β_{mod} and constant relative compliance, (a) $\beta_{mod}=0.0001$, (b) $\beta mod=0.00005$, (c) $\beta_{mod}=0.00001$, (d) $\beta_{mod}=0.000001$.

NH couples the fictitious model (35) to the whole system. The matrices are of N $[2n, f]$, H $[f, (r_{nl} \cdot f)]$, F$[r_{nl} \cdot f, r_{nl} \cdot f]$, $r_{nl} = 2$, order.

In this way the external forces caused by the crack are reconstructed by the estimates of the disturbance vector v(t). An approximation seems to be a disadvantage, but on the other hand this flexibility and robustness 'against' different crack models for simulations of real crack behaviour would in practice characterize this new crack detection method.

Applying (35), the extended system is obtained with the new system matrix $\mathbf{A}_e$,

$$\begin{bmatrix} \dot{\mathbf{x}}(t) \\ \dot{\mathbf{v}}(t) \end{bmatrix} = \underbrace{\begin{bmatrix} \mathbf{A} & \mathbf{NH} \\ \mathbf{0} & \mathbf{F} \end{bmatrix}}_{\mathbf{A}_e} \begin{bmatrix} \mathbf{x}(t) \\ \mathbf{v}(t) \end{bmatrix} + \begin{bmatrix} \mathbf{I} \\ \mathbf{G} \end{bmatrix} \mathbf{b}(t),$$

$$\mathbf{y}(t) = \begin{bmatrix} \mathbf{C} & \mathbf{0} \end{bmatrix} \begin{bmatrix} \mathbf{x}(t) \\ \mathbf{v}(t) \end{bmatrix}. \tag{36}$$

This extended system (36) with the new system matrix $\mathbf{A}_e$ could be observed by the extended state space observer if the system is completely observable (Luenberger [41]). This requires a suitable choice of matrices F, G and H and measurements. The observability of the undamaged turbo rotor with bearings as a linear mechanical system normally is given because of

non-existent decoupled sub-systems. To guarantee the complete observability of the extended system (36), the following condition must be fulfilled:

$$\text{rank} \begin{bmatrix} \lambda \mathbf{I}_{2n} - \mathbf{A} & -\mathbf{NH} \\ \mathbf{0} & \lambda \mathbf{I}_s - \mathbf{F} \\ \mathbf{C} & \mathbf{0} \end{bmatrix} = 2n + s, \tag{37}$$

with $m \geq s$, $(s \geq f)$; this means that there must be equal or more measurements than nonlinearities. The number of approximated nonlinearities mainly depends on the degrees of freedom of the used crack model in equation (4).

The observer essentially consists of a simulated model with a correction feedback of the estimation error between real and simulated measurements,

$$\begin{bmatrix} \dot{\hat{\mathbf{x}}}(t) \\ \dot{\hat{\mathbf{v}}}(t) \end{bmatrix} = \underbrace{\begin{bmatrix} \mathbf{A} - \mathbf{L}_x \mathbf{C} & \mathbf{NH} \\ -\mathbf{L}_v \mathbf{C} & \mathbf{F} \end{bmatrix}}_{\mathbf{A}_o} \begin{bmatrix} \hat{\mathbf{x}}(t) \\ \hat{\mathbf{v}}(t) \end{bmatrix} + \begin{bmatrix} \mathbf{I} \\ \mathbf{G} \end{bmatrix} \mathbf{b} + \begin{bmatrix} \mathbf{L}_x \\ \mathbf{L}_v \end{bmatrix} (\mathbf{y} + \mathbf{w}), \tag{38}$$

where $\mathbf{w}$ represents state measurement noise. The noise vector $\mathbf{w}$ is assumed to be a zero-mean, white random sequence whose covariance is represented by $\mathbf{Rw}$ as follows: $\mathbf{Rw} = E\{\mathbf{ww}^T\}$: positive semidefinite symmetric matrix.

The dynamical behaviour of the observer is expressed by the system matrix $\mathbf{A}_o$. Using an identity observer, different methods can be used like pole-placement or linear-quadratic optimal observer, etc. The asymptotic stability of the observer can be guaranteed by a suitable design of the gain-matrices $\mathbf{L}_x$, $\mathbf{L}_v$. For a successful estimation the observer has to be asymptotically stable and usually the eigenvalues should be on the left side of those of the observed system $\mathbf{A}$. Furthermore the design should consider that only approximations instead of the nonlinearities are used.

According to the presented method the choice of the fictitious model (35) is being effected. Therefore the fictitious model makes sense:

$$\dot{v}_1 = 0, \tag{39}$$

$$\dot{v}_2 = 0, \tag{40}$$

$$\text{i.e.} \quad \mathbf{H} = \begin{bmatrix} 1 & 0 \\ 0 & 1 \end{bmatrix} \alpha \tag{41}$$

$$\mathbf{F} = \begin{bmatrix} 0 & 0 \\ 0 & 0 \end{bmatrix}, \quad \mathbf{v} = \begin{bmatrix} v_1 \\ v_2 \end{bmatrix}, \tag{42}$$

$$h_1(z_{i+1}(t), t) = n_1(x_{2i+1}(t), t) \approx \alpha v_1(t) \tag{43}$$

$$h_2(z_{i+2}(t), t) = n_2(x_{2i+2}(t), t) \approx \alpha v_2(t). \tag{44}$$

The reconstruction of the characteristic relative crack compliance h_r, cf. eq. (6), can be done by simple calculations using the matrix $\mathbf{T}$ (8), the estimated disturbance forces $\hat{v}_{1,2}$ (43, 44), displacements at crack position $(\hat{x}_{2i+1,2i+1})$ (38) and phase information β.
The gain matrices $\mathbf{L}_x$ and $\mathbf{L}_v$ can be chosen by:
- pole assignment methods,
- Riccati observer, which fulfills the following requirements:

$$\mathbf{A}_e \mathbf{P} + \mathbf{P} \mathbf{A}_e{}^T - \mathbf{P} \mathbf{C}^T \mathbf{R}^{-1} \mathbf{C} \mathbf{P} + \mathbf{Q} = 0 \,. \tag{45}$$

Since using approximations instead of the real nonlinearities, the weighting matrices $\mathbf{R}$ and $\mathbf{Q}$ must be chosen specifically. For this the weighting $\mathbf{Q}$ of the measurements is splitted up into three blocks, like

$$\mathbf{Q} = \begin{bmatrix} q_1 \mathbf{I}_n & 0 & 0 \\ 0 & q_2 \mathbf{I}_n & 0 \\ 0 & 0 & q_3 \mathbf{I}_{r_{nl} \cdot f} \end{bmatrix}. \tag{46}$$

The weighting matrix $\mathbf{R}$ in equation (38) is

$$\mathbf{R} = r \, \mathbf{I}_m. \tag{47}$$

4.3. CRACK DETECTION BY STATE OBSERVERS

Crack detection by state observers means a procedure with three steps:
1. Estimation of crack forces $\hat{\mathbf{v}}(t)$ via the extended state space observer.
2. Recalculating the coefficients of $\mathbf{K}_e\,(\check{\mathbf{z}}\,(t)\,,t)$ (4) or e.g., $\mathbf{h}_{chcr}\,(\check{\mathbf{z}}\,(t))$ (3) for each time step and representing them in a favourable manner, e.g., dividing by the nominal values of the undamaged case. Therefore phase information is useful.
3. Consideration of noise measurements and stochastical errors.

The numerical values were chosen to generate measurement signals with 40, 26 and 20 dB signal to noise (S/N) ratio. Figures 6 and 7 show the mechanical forces F_n in the horizontal direction and relative crack compliance h_r for crack depth $t_r = 10\%$, where $t_r = \frac{t}{r}$, t - crack depth and r - radius of the rotor at crack position. In Figure 6 results are shown using pole assignment method and in Figure 7 using Riccati observer with $q_1 = 1$, $q_2 = 1$, $q_3 = 10^9$ and r = 0.001.

In both cases it was noticed that elements of the gain matrices $\mathbf{L}_x$ and $\mathbf{L}_v$ were too large, so the observer became sensitive with respect to noisy measurements. Therefore we have applied Riccati observer with $q_1 = q_2 = 1, q_3 = 300$ and r = 0.01. The effects of the measurement noise on the estimated 'crack forces' in the horizontal direction are shown in Figures 8, 9, and 10, for the relative crack depths $t_r = 0, 10$ and 20% respectively.

The observer estimates the signal very well, only in a few points the dynamics of the observer cannot follow the real simulated signal. The external signal only exists if the crack opens, and the maximal values depend on the crack depth. Using this estimation and the estimation about the displacements, the normally unknown ratio $h_r = \frac{h_a}{h}$ in (6) can be recalculated, Figure 11. As a function of time this ratio describes the variable compliance or stiffness depending on the phase angle in the rotating coordinate system. Hence it will be a clear indicator for cracks. Here the opening and closing of the crack is shown very clearly and unambiguously. For both crack depths it is very clear to see opening and closing of the crack in the crack model of Gasch. In contrast to this the calculations of the undamaged rotor results in a ratio about 0.001.

5. Summary and Conclusions

This work investigates the nonlinear dynamics of a cracked rotor. Due to the crack, which causes a change in stiffness coefficients, the system becomes a parameter excited and nonlinear
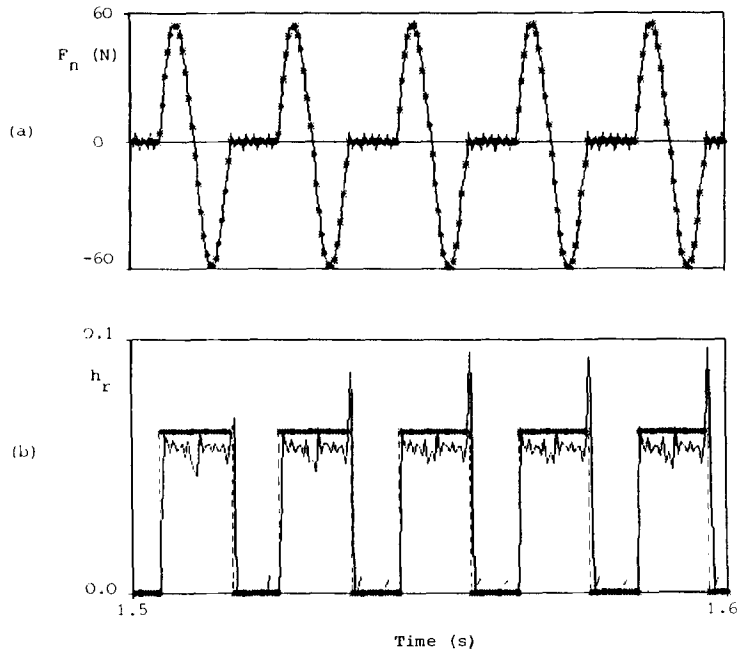
Fig. 6. (a): Reconstructed crack forces $\hat{v}_2$ at the crack position ($t_r = 10\%$), (b): recalculated relative crack compliance h_r; using pole assignment method, (****** simulation result, ——— reconstruction/recalculation).

one (with discontinuities caused by transition between motion with closed crack and motion with open crack). To examine the behaviour of the system beside phase plane plots, Poincaré maps, time histories and power spectrum, the linearized equations of motion and transition conditions were obtained and the greatest Lyapunov exponent was calculated. Depending on the relative crack compliance h_r, we can obtain different types of motions: sub- or ultrasubharmonic, quasiperiodic, fractal-like torus or chaotic ones.

A detailed study of the vibrational behaviour of a cracked rotating shaft is an important problem for engineers working in the area of the dynamics of machines, and an early warning can considerably extend the durability of those expensive machines, increasing their reliability at the same time. Therefore a new observer-based method has been developed and applied to a turbo-rotor. This method gives a clear relation between shaft cracks and caused phenomena in vibrations measured in bearings. Simulations have been done, showing the theoretical success of this method, especially for reconstructing disturbance forces as inner forces caused by a crack. Calculating the relative crack compliance as the ratio of additional compliance caused by the crack and undamaged compliance, a clear statement about the opening and closing, and therefore for the existence of the crack, and about the crack depth is possible. Theoretically it has been shown that it is possible to detect a crack with very small stiffness changes which corresponds to a crack depth of 10 % of the radius of the rotor. The results are nearly the same if noise measurements are considered. To what extent this success can be transferred into practice has to be analyzed by further investigations and experiments.
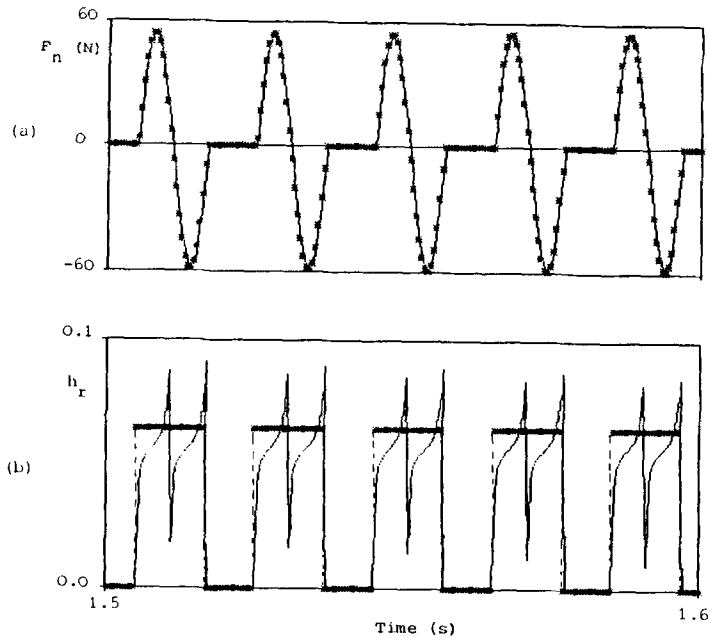
Fig. 7. (a): Reconstructed crack forces $\hat{v}_2$ at the crack position ($t_r = 10\%$), (b): recalculated relative crack compliance h_r; using Riccati observer, $q_1 = q_2 = 1$, $q_3 = 10^9$, $r = 0.001$, (****** simulation result, ———— reconstruction/recalculation).

Acknowledgement

Appendix

The matrices used in Equations (1) and (5) are as follows,

M : Mass matrix of order (16 × 16),

$$\mathbf{M} = \text{diag} \left[\frac{m}{2} \ \frac{m}{2} \ \underbrace{m \ \ldots \ldots \ m}_{12 \text{ times}} \ \frac{m}{2} \ \frac{m}{2} \right], \tag{48}$$

where $m = \pi r^2 l \, \varrho$, $\varrho = 7860 \ kg/m^3$,

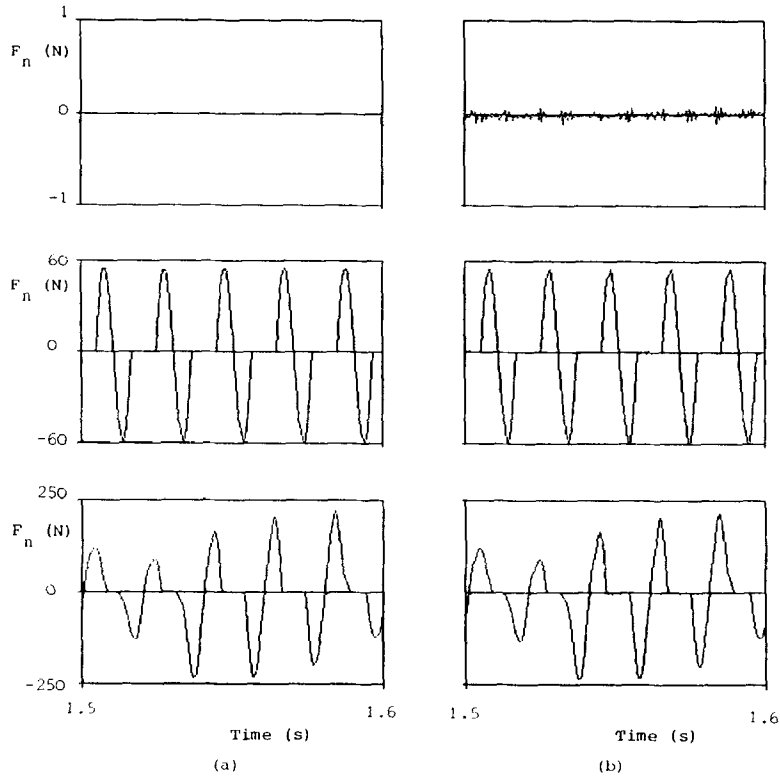**K** : Stiffness matrix of order (16 × 16),

Fig. 8. Reconstructed crack forces $\hat{v}_2$ at the crack position ($t_r = 0\%, 10\%$, and 20% respectively), (a): $\mathbf{w} \equiv \mathbf{0}$, (b) with 40 dB S/N ratio in measurements; using Riccati observer, $q_1 = q_2 = 1, q_3 = 300, r = 0.01$.

$$
\mathbf{K} = \begin{bmatrix}
k_1 & 0 & k_3 & 0 & 0 & 0 & \ldots & \ldots & \ldots & 0 \\
0 & k_1 & 0 & k_3 & 0 & 0 & \ldots & \ldots & \ldots & 0 \\
k_3 & 0 & k_2 & 0 & k_3 & 0 & \ldots & \ldots & \ldots & 0 \\
0 & k_3 & 0 & k_2 & 0 & k_3 & \ldots & \ldots & \ldots & 0 \\
\vdots & & & & & & & & & \\
\vdots & & & & & & & & & \\
0 & \ldots & \ldots & \ldots & k_3 & 0 & k_2 & 0 & k_3 & 0 \\
0 & \ldots & \ldots & \ldots & 0 & k_3 & 0 & k_2 & 0 & k_3 \\
0 & \ldots & \ldots & \ldots & 0 & 0 & k_3 & 0 & k_1 & 0 \\
0 & \ldots & \ldots & \ldots & 0 & 0 & 0 & k_3 & 0 & k_1
\end{bmatrix}
\tag{49}
$$

where $k = 12\,E\,J/l^3$, $E = 2.1 \cdot 10^5\,N/mm^2$, $k_s = 7.5 \cdot 10^5\,N/mm$,
$\quad k_1 = k + k_s$, $k_2 = 2\,k$, $k_3 = -k$,

$\mathbf{D}$: Damping matrix of order (16×16),

$$
\mathbf{D} = \beta_{mod} \cdot \mathbf{K}, \quad \beta_{mod} = 0.00001,
\tag{50}
$$

$\mathbf{f}$: Vector of unbalances of order (16×1),
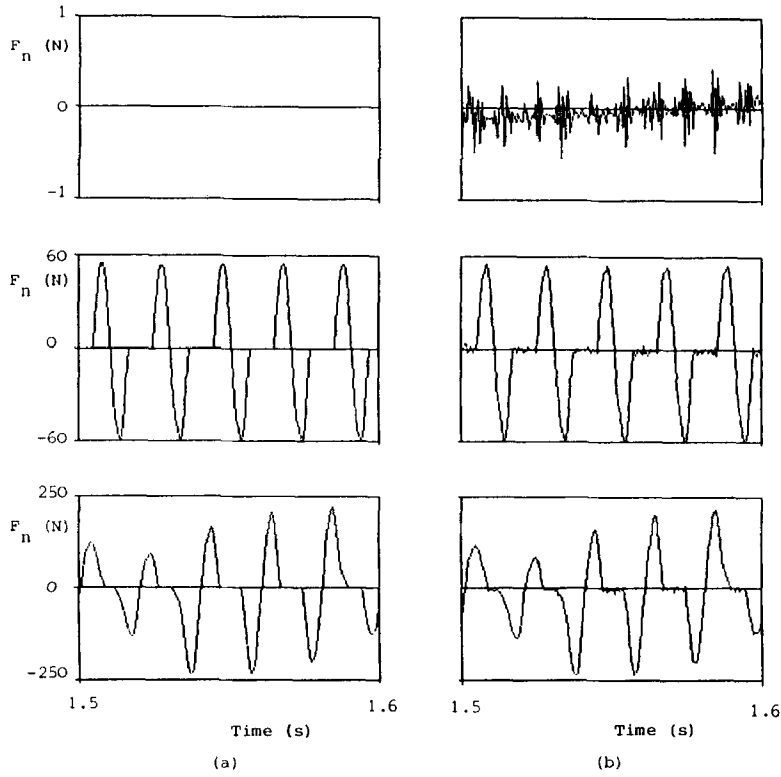
$$
f_{2i} = 0, \quad i = 1, 2, \ldots, 8, \quad \text{except}
$$

Fig. 9. Reconstructed crack forces $\hat{v}_2$ at the crack position ($t_r = 0\%$, 10%, and 20% respectively), (a): $\mathbf{w} \equiv \mathbf{0}$, (b) with 26 dB S/N ratio in measurements; using Riccati observer, $q_1 = q_2 = 1$, $q_3 = 300$, $r = 0.01$.

$$f_1 = f_{15} = -mg/2,$$
$$f_3 = f_5 = f_7 = f_9 = f_{13} = f_{15} = -mg, \tag{51}$$
$$f_{11} = -mg + e_m \Omega^2 m_{ex} \sin(\Omega t + \beta),$$
$$f_{12} = e_m \Omega^2 m_{ex} \sin(\Omega t + \beta - 90°),$$

where $m_{ex} = 7m$ — the mass of eccentricity, $\beta = 0°$,

$\mathbf{N}_n$: Matrix of nonlinearities of order (16×2),

$$n_{n71} = n_{n82} = 1, \tag{52}$$

the remaining elements are zero,

$\mathbf{h}$: Vector of the crack forces of order (2×1),
in the case of the 'closed' crack, i.e. if $\chi \leq 0$ in Eq. (7), than $\mathbf{h} \equiv \mathbf{0}$.
in the case of the 'open' crack, i.e. if $\chi > 0$ in Eq. (7),
or in the inertial coordinate frame

$$z_7 \cos(\Omega t + \beta) + z_8 \sin(\Omega t + \beta)$$
$$> \frac{[(z_5 + z_9)\cos(\Omega t + \beta) + (z_6 + z_{10})\sin(\Omega t + \beta)]}{2}, \tag{53}$$
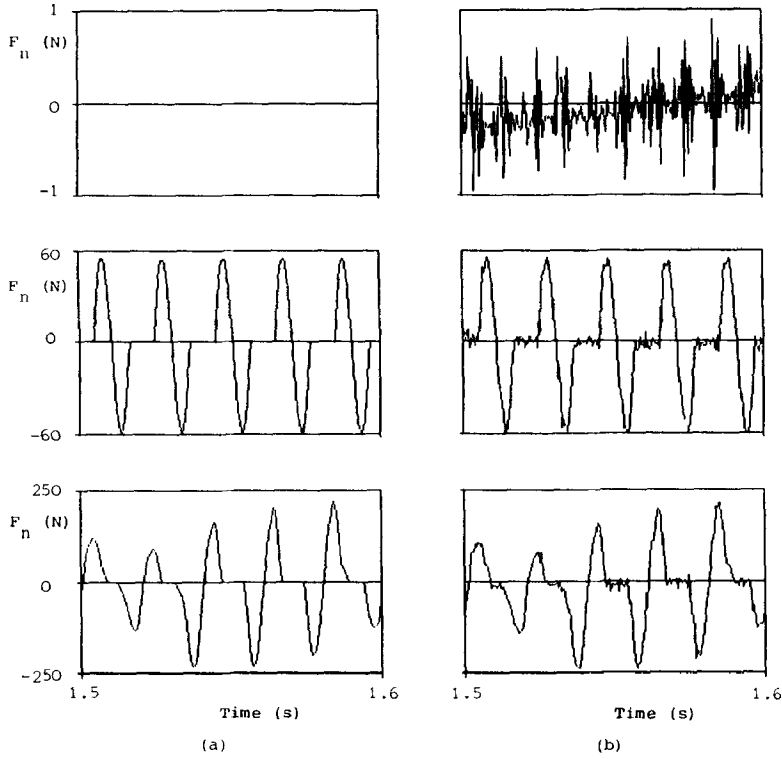
Fig. 10. Reconstructed crack forces $\hat{v}_2$ at the crack position (t_r = 0%, 10%, and 20% respectively), (a): $\mathbf{w} \equiv \mathbf{0}$, (b) with 20 dB S/N ratio in measurements; using Riccati observer, $q_1 = q_2 = 1$, $q_3 = 300$, $r = 0.01$.

then the elements of the (2×1) vector $\mathbf{h}$ are as follows:

$$h_1 = [-z_7 \cos^2(\Omega t + \beta) - z_8 \sin(\Omega t + \beta) \cos(\Omega t + \beta)] \frac{k_2 h_r}{1 + h_r},$$

$$h_2 = [-z_8 \sin^2(\Omega t + \beta) - z_7 \sin(\Omega t + \beta) \cos(\Omega t + \beta)] \frac{k_2 h_r}{1 + h_r},$$

(54)

all other elements are zero,

$\mathbf{A}$: The system matrix of order (32×32),

$$\mathbf{A} = \begin{bmatrix} \mathbf{0} & \mathbf{I}_n \\ -\mathbf{M}^{-1}\mathbf{K} & -\mathbf{M}^{-1}\mathbf{D} \end{bmatrix},$$

(55)

$\mathbf{b}$: Vector of excitation of order (32×1),

$$\mathbf{b} = \begin{bmatrix} \mathbf{0} \\ \mathbf{M}^{-1}\mathbf{f} \end{bmatrix},$$
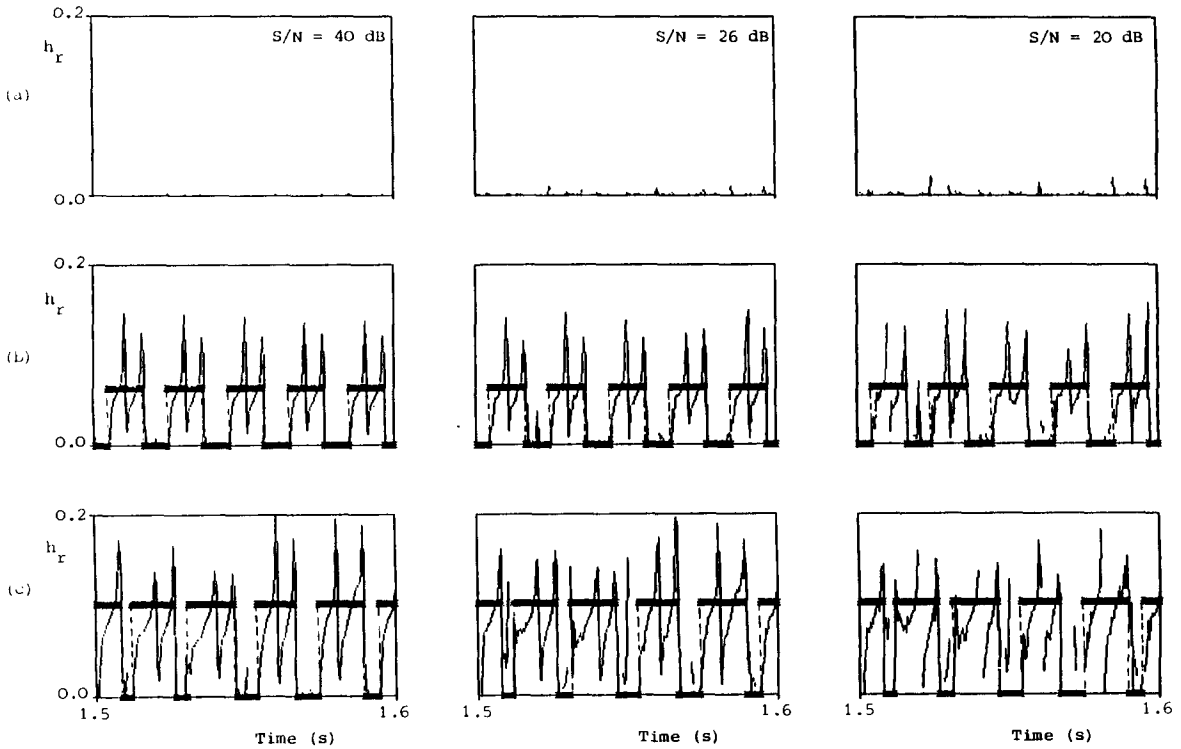
(56)

Fig. 11. Recalculated relative crack compliance h_r using Ricatti observer, $q_1 = q_2 = 1$, $q_3 = 300$, $r = 0.01$; at the crack position, (a) $t_r = 0\%$, (b) $t_r = 10\%$, and (c) $t_r = 20\%$, for different S/N ratio in measurement, respectively 40, 26 and 20 dB.

N : Matrix of nonlinearities of order (32 × 2),

$$N = \begin{bmatrix} \mathbf{0} \\ -\mathbf{M}^{-1}\,\mathbf{N}_n \end{bmatrix}, \tag{57}$$

n : Vector of nonlinear functions of order (2 × 1),
in the case of the 'closed' crack $\mathbf{n} \equiv \mathbf{0}$,
in the case of the 'open' crack,

$$n_1 = [-x_7 \cos^2(\Omega t + \beta) - x_8 \sin(\Omega t + \beta)\,\cos(\Omega t + \beta)]\,\frac{k_2\,h_r}{1 + h_r},$$

$$\tag{58}$$

$$n_2 = [-x_8 \sin^2(\Omega t + \beta) - x_7 \sin(\Omega t + \beta)\,\cos(\Omega t + \beta)]\,\frac{k_2\,h_r}{1 + h_r},$$

C : Measurement matrix of order (8 × 32),

$$c_{ij} = 0, \quad i = 1, 2, \ldots, 8, \quad j = 1, 2, \ldots, 32, \quad \text{except} \tag{59}$$

$$c_{11} = c_{22} = c_{3,15} = c_{4,16} = c_{5,17} = c_{6,18} = c_{7,31} = c_{8,32} = 1\,.$$

References

1. Szczygielski, W. M., 'Dynamisches Verhalten eines schnell drehenden Rotors bei Anstreifvorgängen', Dissertation, ETH Zürich, Nr. 8094, 1986.
2. Bajkowski, J. and Müller, P. C., 'Lyapanov exponents and fractal dimensions in nonlinear mechanical systems', *Zeitschrift für Angewandte Mathematik und Mechanik* **68**, 1988, 49–53.
3. Moon, F. C. and Shaw, S. W., 'Chaotic vibrations of a beam with nonlinear bounding excitations', *International Journal of Non-Linear Mechanics* **18**, 1983, 465–477.
4. Pfeiffer, F., 'Seltsame Attraktoren in Zahnradgetrieben', *Ingenieur -Archiv* **58**, 1988, 113–125.
5. Pater, A. D. de, 'The lateral behaviour of railway vehicles', in Schiehlen, W.O. (ed.) *Dynamics of High Speed Vehicles*, Springer-Verlag, Wien, 1982.
6. Pater, A. D. de, 'Optimal design of running gears', *Vehicles Systems Dynamics* **18**, 1989, 293–299.
7. Meijaard, J. P., 'Dynamics of mechanical systems', Dissertation, Technical University Delft, 1991.
8. Jansen, J. D., 'Nonlinear rotor dynamics applied to oilwell drillstring vibrations', *Journal of Sound and Vibration* **147**, 1991, 115–135.
9. Paidoussis, M. P. and Moon, F. C., 'Nonlinear and chaotic fluidelastic vibrations of a flexible pipe conveying fluid', *Journal of Fluids and Structures* **2**, 1988, 567–591.
10. Popp, K. and Stelter, P., 'Nonlinear oscillations of structures induced by dry friction', in Schiehlen, W. O. (ed.) *Nonlinear Dynamics in Engineering Systems*, Springer-Verlag, Berlin, 1990.
11. Stelter, P., 'Nichtlineare Schwingungen reibungserregter Strukturen', VDI-Fortschrittsberichte Nr. 137, Reihe 11, VDI-Verlag, Düsseldorf, 1990.
12. Fritzen, C. P., 'Reguläres und chaotisches Verhalten einer Laval-Welle mit Riss', *Zeitschrift für Angewandte Mathematik und Mechanik* **70**, 1990, 112–114.
13. Müller, P. C., Bajkowski, J. and Kisljakov, S. D., 'Model based calculation of Lyapunov exponents for dynamic systems with discontinuities', *2nd Polish-German Workshop on Dynamical Problems in Mechanical Systems*, March 10–17, Paderborn, Germany, 1991.
14. Söffker, D. and Bajkowski, J., 'Crack detection by state observers', in *Proceedings of the 8th IFToMM World Congress on the Theory and Practice of Machines and Mechanisms*, Prague, 1991, 771–774.
15. Söffker, D., Bajkowski, J., and Müller, P. C., 'Detection of cracks in turbo rotors – a new observer based method', *ASME Journal of Dynamic Systems, Measurements and Control*, **15**, 1993, 518–524 .
16. Zimmer, S. and Bently, D. E., 'Predictive maintenance programs for rotating computerized vibration monitoring systems', VDI-Berichte 568, VDI-Verlag, Düsseldorf, 1985, 265–287.
17. Peter, U., 'Schwingungsüberwachung an großen Turbosätzen - Stand und sinnvolle Weiterentwicklung aus Betreibersicht', VDI-Berichte 568, VDI-Verlag, Düsseldorf, 1985, 105–125.
18. Ericsson, U., 'Vibration monitoring – the state of the art – with case studies', VDI-Berichte 568, VDI-Verlag, Düsseldorf, 1985, 289–303.
19. Gasch, R., 'Dynamic behaviour of a simple rotor with a cross-sectional crack', *Vibrations in Rotating Machinery*, Institution of Mechanical Engineers, London, 1976, 123–128.
20. Henry, T. A. and Okah-Avae, B. E., 'Vibrations in cracked shafts', *Vibrations in Rotating Machinery*, Institution of Mechanical Engineers, London, 1976, 15–19.
21. Mayes, I. W. and Davies, W. G. R., 'A method of calculating the vibrational behaviour of coupled rotating shafts containing a transverse crack', *Vibrations in Rotating Machinery*, Institution of Mechanical Engineers, London, 1980, 17–27.
22. Grabowski, B. and Mahrenholtz, O., 'Theoretical and experimental investigations of shaft vibrations in turbomachinery excited by cracks', *Proceedings of International Conference on Rotordynamic Problems in Power Plants*, IFToMM, Rome, 1982, 507–514.
23. Bently, D., 'Breakthroughs made in observing crack shafts', *Orbit* **2**, 1981.
24. Bently, D., 'Detecting crack shafts at earlier level', *Orbit* **3**, 1982.
25. Muszynska, A., 'Shaft crack detection', *Proceedings 7th Machinery Dynamics Seminar*, Edmonton, 1982.
26. Schmalhorst, B., 'Experimentelle und theoretische Untersuchungen zum Schwingungsverhalten angerissener Rotoren', VDI-Fortschrittsberichte Nr. 117, Reihe 11, VDI-Verlag, Düsseldorf, 1989.
27. Wauer, J., 'On the dynamics of cracked rotors: A literature survey', *Applied Mechanics Reviews* **43**, 1990, 13–17.
28. Papadopoulos, C. A. and Dimarogonas, A. D., 'Coupled longitudinal and bending vibrations of a rotating shaft with an open crack', *Journal of Sound and Vibration* **117**, 1987, 81–93.
29. Dimarogonas, A. D. and Papadopoulos, C. A., 'Vibrations of shaft cracks in bending', *Journal of Sound and Vibration* **91**, 1983, 583–593.

30. Müller, P. C., 'Indirect measurements of nonlinear effects by state observers', *IUTAM Symposium on Non-linear Dynamics in Engineering Systems, University of Stuttgart*, Springer-Verlag, Berlin, 1990, 205–215.

31. Mayes, I. W. and Davies, W. G. R., 'Analysis of the response of a multi-rotor-bearing system containing a transverse crack in a rotor', *Journal of Vibration, Acoustics, Stress and Reliability in Design*, paper no 83 DET 84, 1984, 139–145.

32. Moon, F. C., *Chaotic Vibrations, an Introduction for Applied Scientists and Engineers*, Wiley, New York, 1987.

33. Lichtenberg, A. J. and Lieberman, M. A., *Regular and Stochastic Motion*, Springer-Verlag, New York, 1983.

34. Oseledec, V. I., 'A multiplicative ergodic theorem. Ljapunov characteristic numbers for dynamical systems', *Transactions Moscow Mathematical Society* **19**, 1968, 197–231.

35. Eckmann, J-.P. and Ruelle, D., 'Ergodic theory of chaos and strange attractors', *Reviews of Modern Physics* **57**, 1985, 617–656.

36. Haken, H., 'At least one Lyapunov exponent vanishes if the trajectory of an attractor does not contain a fixed point', *Physics Letters* **94A**, 1983, 71–72.

37. Wolf, A., Swift, J. B., Swinney, H. L., and Vastano, J. A., 'Determining Lyapunov exponents from a time series', *Physica* **16 D**, 1985, 285–317.

38. Shimida, I. and Nagashima, T., 'A numerical approach to ergodic problem of dissipative dynamical systems', *Progress of Theoretical Physics* **61**, 1979, 1605–1616.

39. Benettin, G., Galgani, A., Giorgilli, A., and Strelcyn J.-M., 'Lyapunov characteristic exponent for smooth dynamical systems and for Hamiltonian systems; a method for computing all of them. Part I: Theory. Part II: Numerical application', *Meccanica* **15**, 1980, 9–30.

40. Munteau, G. G. and Moon, F. C., 'Multifractals in flow-induced vibrations', Tenth Symposium on Energy Engineering Sciences, Aragonna National Laboratory, Aragonna, Illinois, May 11–13, 1992.

41. Luenberger, D. G., 'An introduction to observers', *IEEE Transactions of Automatic Control* **AC-16**, 1971, 596–602.